Penerbit Akademia Baru

Journal of Advanced Research Design

Journal homepage:
https://akademiabaru.com/submit/index.php/ard
ISSN: 2289-7984

Performance of Hyperthermia Applicator under ISM Frequency for Breast Cancer Treatment

Bibi Sarpinah Sheikh Naimullah[1,2*], Kasumawati Lias[1], Ahmad Tirmizi Jobli[3], Mazlina Mansor Hassan[1,2], Fatimatul Anis Bakri[1], Muhd Firdaus Muhd Yusoff[1]

[1] Department of Electrical and Electronics Engineering, Faculty of Engineering, Universiti Malaysia Sarawak(UNIMAS),94300, Kota Samarahan, Sarawak, Malaysia
[2] Electrical Engineering Studies, College of Engineering, Universiti Teknologi MARA,94300, Kota Samarahan, Sarawak, Malaysia
[3] Faculty of Medicine and Health Sciences, Universiti Malaysia Sarawak,94300 Kota Samarahan, Sarawak, Malaysia

ARTICLE INFO

Article history:
Received 16 April 2025
Received in revised form 14 July 2025
Accepted 23 September 2025
Available online 1 October 2025

Keywords:
Hyperthermia; SAR; Penetration depth; Applicator; Breast phantom

ABSTRACT

Hyperthermia is a treatment procedure that applies heat on the target tissue with a temperature range of 40º to 45º C for a specific duration without affecting the healthy surrounding tissue. The efficacy of hyperthermia treatment relies on the suitable frequency within the Industrial, Scientific, and Medical (ISM) band. The frequency influences both penetration depth and Specific Absorption Rate. This study aims to investigate and compare the performance of the applicator with operating frequencies 434MHz, 915MHz, and 2450MHz with a tumor situated in the middle of the breast phantom. The hyperthermia model is simulated with SEMCAD X. Tissue properties include relative permittivity and conductivity represented with the Generic Dispersive Model. The penetration SAR distribution varies with different frequencies applied to the applicator. The applicator with 434MHz has greater penetration than 915MHz and 2450MHz. The SAR distribution on 2450MHz is more focused on the areola of the breast phantom, while on 915MHz, heat focuses on the middle of the breast phantom. For applicator 434MHz, the heat covers the middle part of the breast phantom to the chest wall. The appropriate applicator is recommended for effective hyperthermia treatment.

1. Introduction

The most widely used cancer treatments globally are surgery, chemotherapy and radiation therapy. Nevertheless, specific pathological characteristics in the tumor can reduce the effectiveness of the available treatment. For example, a hypoxic tumor is characterized by low oxygen level (PO2) [1] and disorganized blood vessel development due to insufficient blood supply[2]. Hypoxia induces an increase in malignancy [3] and resistance to chemotherapy and radiation therapy[4]. Therefore, hyperthermia is an option for this type of tumor treatment.

Hyperthermia is defined as the elevation of tissue temperature from 40º to 45º C for 30 to 60 minutes while causing a minimal effect on the healthy surrounding tissue[5]. The increment in

* *Corresponding author.*
E-mail address: sarpinah187l@gmail.com

https://doi.org/10.37934/ard.145.1.112

temperature leads to the destruction of cell cancer. Hyperthermia can be independent or in conjunction with chemotherapy and radiation therapy to increase its effectiveness[6].

In hyperthermia treatment, an applicator generates heat that transfers it to tissue. In healthy tissue, this heat causes an increase in blood flow because of blood vessel enlargement. This response helps to keep the temperature lower in healthy tissue. However, in the tumor, blood flow slows down due to the abnormal structure of blood vessels. As a result, the temperature in the tumor rises, leading to cell death or shrinkage of the cancer due to heat exposure [7].

Clinical heating techniques are electromagnetic (EM), ultrasound, perfusion and conductive heating. The EM heating applies a frequency alternating sinusoidal (AC) EM field generated through one or multiple antenna. The antenna/multiple antenna is called the applicator. The EM field induces dielectric heating through molecular dipole rotation, polarization or vibration. At a frequency >1MHz, the cell membrane allows the electric field to pass through and make it permeable[8]. EM method can be categorized based on frequency, wavelength and penetration depth. The ascending order of frequency corresponds to the descending order of penetration depth[9].

The interaction between the EM field and biological tissue is commonly investigated through a comprehensive model, including dielectric properties. The dielectric properties are relative permittivity and electrical conductivity[10]. Electrical conductivity refers to the material/tissue's ability to carry current. Healthy tissue and tumors have different electrical conductivity[11]. The relative permittivity describes the ability of material/tissue to be polarised due to the EM field. Both electrical properties are subject to the type of tissue, frequency and temperature[12].

The hyperthermia applicator utilized frequency within the range designated by Industrial, Scientific and Medical (ISM) at 434MHz, 915MHz and 2450MHz[13]. The applicator used the ISM band to reduce the complications and cost-effective device installation in the clinic[14]. A previous study reported that the frequency utilized in the applicator design influenced the penetration depth. Penetration depth at high frequency is lesser than at low frequency. For instance, in [15], an applicator utilized 434MHz to treat locally advanced breast cancer, while [16] demonstrated that 434MHz provided greater penetration depth than 915MHz and 2450MHz.

Additionally, [14] indicated that applicator 915MHz has a more prominent focus point and deeper penetration depth than 2450MHz. Meanwhile, the 2450MHz applicator resulted in more focus on treatment but with reduced penetration depth[17]. The variation of penetration depth indicates the efficacy of tumor treatment depends on the frequency used in the applicator. Therefore, this study proposed an applicator that allows precise tumor treatment by selecting an appropriate operating frequency based on tumor location.

2. Methodology

The SEMCAD X is a 3D full-wave EM simulation with Finite Difference Time Domain (FDTD) method. The FDTD method simulates EM behavior by numerically solving the Maxwell equation in discrete space and time domains. The Yee grid scheme provides an effective framework for discretizing and solving the Maxwell equation for the numerical modeling of EM waves. Through Faraday and Ampere law with Maxwell addition[18], electric field (Ex, Ey, Ez) and magnetic field (Hx, Hy, Hz) are placed on a grid system in Cartesian coordinates. These field components are positioned at a staggered grid [19]. The equation fundamental of EM wave. Maxwell Eq. (1) Faraday Law explains how the change in magnetic field induces an electric field.

$$\nabla xE = -\frac{\partial}{\partial t}\mu H \tag{1}$$

Ampere law with Maxwell addition is shown in Eq. (2), which explains how the magnetic field is related to the electric field and current density. Maxwell introduced the concept of displacement current that allows direct proportional to the rate of change of electric field, $\frac{\partial}{\partial t}E$ as in Eq. (2a)

$$\nabla \mathrm{x} \mathrm{H} = \frac{\partial}{\partial t}\varepsilon E + J \tag{2}$$

$$\nabla \mathrm{x} \mathrm{H} = \frac{\partial}{\partial t}\varepsilon E + \ \sigma E \tag{2a}$$

Rearrange (2a)

$$\frac{\partial E}{\partial t}\varepsilon = \ \nabla \mathrm{x} \mathrm{H} - \sigma E \tag{2b}$$

$$\frac{\partial E}{\partial t}\varepsilon = \ \frac{1}{\varepsilon}(\nabla \mathrm{x} \mathrm{H} - \sigma E) \tag{2c}$$

At XY grid cell, Ex with Hy and Hz as:

$$\frac{\partial E}{\Delta t} = \ \frac{1}{\varepsilon}\left(\frac{H_z}{\Delta y}\frac{-H_y}{\Delta z} - \sigma E\right) \tag{2d}$$

In the context of solving electrical problems with the FDTD method. By assuming from electric field (Ex) change from time step (n) to the subsequent step (n+1) in the X and Y grid, magnetic field (Hz and Hy) at spatial interval along grid Δy and Δz shift by half of the grid point in both X and Y direction as indicated in Figure 1. Meanwhile, the conductivity is at a specific location in the grid[20]. It shows that the electric field changes based on the magnetic field and material conductivity, as in (2e).

$$\frac{Ex_{n+1} - Ex_n}{\Delta t} = \ \frac{1}{\varepsilon}\left(\frac{Hz_{n+\frac{1}{2}}}{\Delta y} - \frac{Hy_{n+\frac{1}{2}}}{\Delta z} - \sigma E\right) \tag{2e}$$

By considering specific locations within the grid (i,j,k), Ex stated as:

$$\frac{Ex|_{n+1(i,j,k)} - Ex|_{n(i,j,k)}}{\Delta t} = \tag{2f}$$

$$\frac{1}{\varepsilon_{(i,j,k)}}\left[\frac{Hz|_{n+\frac{1}{2}\left(i,j+\frac{1}{2},k\right)} - Hz|_{n+\frac{1}{2}\left(i,j-\frac{1}{2},k\right)}}{\Delta y} - \frac{Hy|_{n+\frac{1}{2}\left(i,j,k+\frac{1}{2}\right)} - Hy|_{n+\frac{1}{2}\left(i,j,k-\frac{1}{2}\right)}}{\Delta z} - \sigma_{(i,j,k)} Ex|_{n+\frac{1}{2}(i,j,k)}\right]$$

Assume Ex position at half grid point of the XY :

$$Ex_{n+\frac{1}{2}} = \frac{Ex_n + Ex_{n+1}}{2} \tag{2g}$$

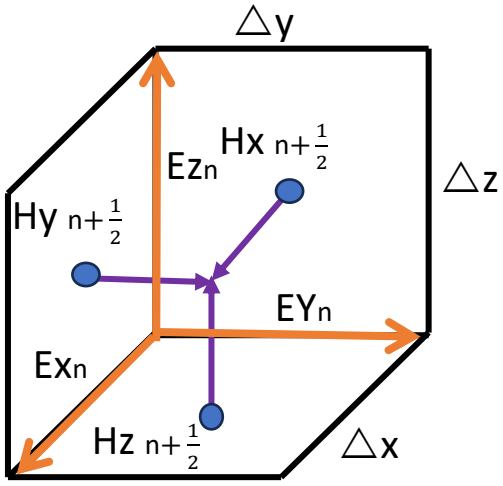

Fig. 1. Yee Cell in the electric and magnetic field in a staggered grid (FDTD)

Sections 2.1, 2.2, and 2.3 describe the applicator development, breast phantom development, and Specific Absorption Rate , respectively.

2. 1 Applicator Development

The applicator was designed with a rectangular microstrip antenna that used RT5880 as the substrate with an input power of 10W. Developing the antenna with an RT5880 substrate improved several performance aspects, including reduced return loss, increased gain, enhanced directivity, and improved efficiency [21]. Besides that, RT5880 has low loss a tangent and low loss dielectric constant, which are essential for microstrip antenna.

The size of a rectangular microstrip antenna with 434MHz is 349.31(*l*) x 282.50(*w*) x 1.575(*h*) mm^3. The patch dimension is 231.79(l) x 273.79(w) x 0.035(h) mm^3, as displayed in Figure 2a. The size of a rectangular microstrip antenna with 915MHz is 166.68*(l)* x 138.96*(w)* x 1.575*(h)* mm^3. The patch dimension is 110.39(l) x 129.51(w) x 0.035(h) mm^3, as indicated in Figure 2b. The size of a rectangular microstrip antenna with 2450MHz is 49.473*(l)* x 57.819*(w)* x 1.575*(h)* mm^3. The patch dimension is 40.02*(l)* x 48.37*(w)* x 0.035*(h)* mm^3 as shown in Figure 2c.

The dimension length and width are based on governing equations[22] that represent in steps 1 to 6. The thickness substrate RT5880 and patch-based datasheet[23]. The substrate has a dielectric constant, $\varepsilon_r = 2.2$ and loss tangent tanδ=0.0009[24]. Microstrip line used as feeding method the feed line is $\frac{\lambda}{4}$. The transmission line impedance is 50 Ω.

Step 1: width of patch for rectangular microstrip antenna

$$W_p = \frac{c}{2f_r}\sqrt{\frac{2}{\varepsilon_r + 1}} \tag{3}$$

Step2: The effective dielectric constant of the substrate

$$\varepsilon_{reff} = \frac{\varepsilon_r + 1}{2} + \frac{\varepsilon_{r-1}}{2}\left[1 + 12\frac{h}{w}\right]\left[1 + 12\frac{h}{w}\right]^{-0.5} \quad (4)$$

Step 3: The effective length of the microstrip antenna

$$L_{eff} = \frac{c}{2f_r\sqrt{\varepsilon_{reff}}} \quad (5)$$

Step 4: The extension of length

$$\Delta L = 0.412h\frac{(\varepsilon_{reff} + 0.3)(\frac{w}{h} + 0.264)}{(\varepsilon_{reff} - 0.258)(\frac{w}{h} + 0.8)} \quad (6)$$

Step 5: The microstrip antenna length

$$L = L_{eff} - 2\Delta L \quad (7)$$

Step 6: The length and width of the ground plane

$$L_{g=}6h + L \quad (8)$$

$$W_{g=}6h + W_p \quad (9)$$

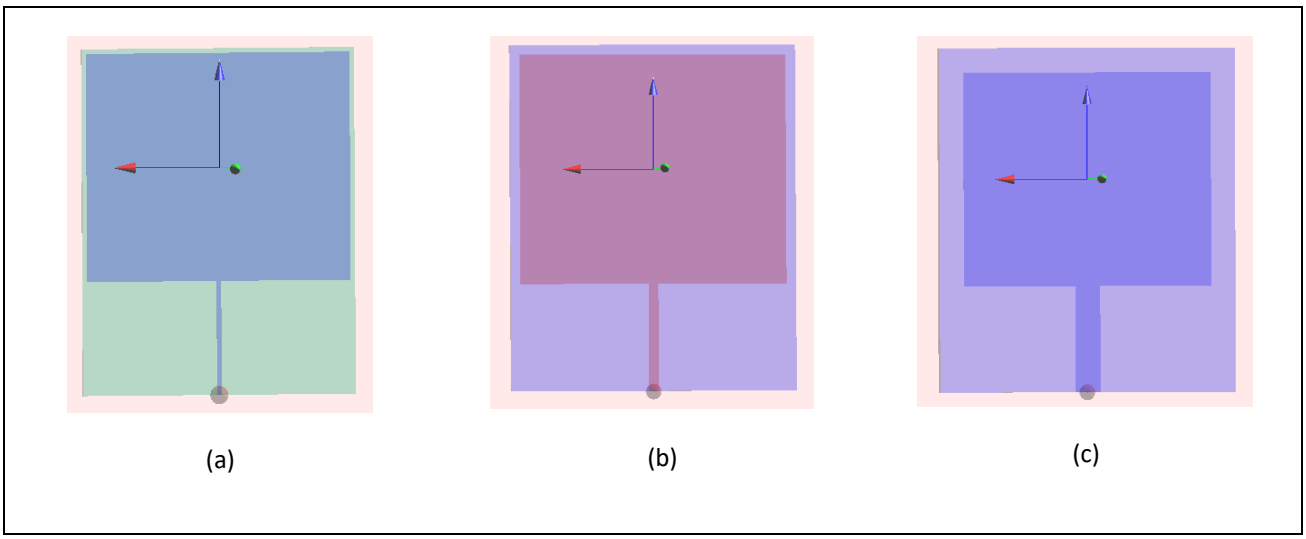

Fig. 2. (a)434MHz Applicator (b) 915MHz Applicator (c) 2450MHz Applicator

2.2 Breast Phantom

A numerical breast phantom with a radius of 95mm develops in SEMCAD with vital tissue layers such as breast fat, tumor and chest muscles, as illustrated in Figure 3. The tumor's location is in a bounding box that provides minimum (P1) and maximum(P2) in (x,y,z) coordinates. P1 and P2 are indicated as in Eq. (10).

$$P\ (x,y,z) = \begin{cases} x: -16 \le x \le 16 \\ y: \ \ 48 \le y \le 80 \\ z: -16 \le z \le 16 \end{cases} \quad (10)$$

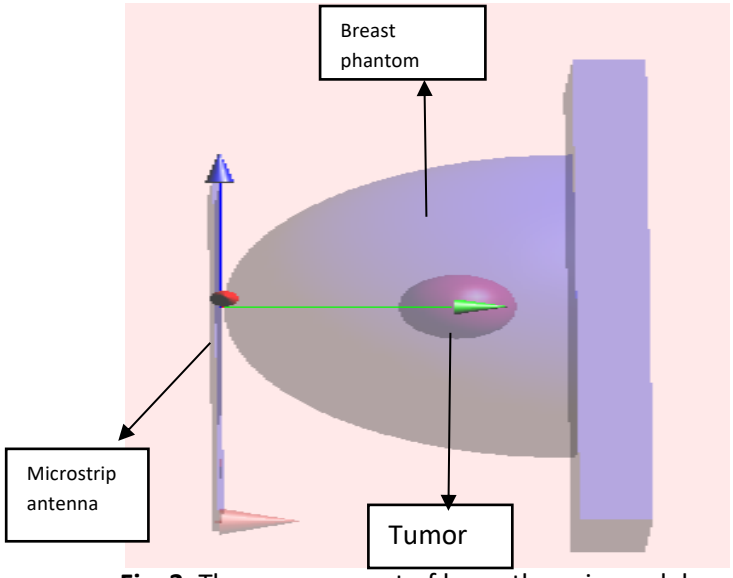

Fig. 3. The arrangement of hyperthermia model

The tumor has higher relative permittivity than breast fat under all frequencies, as indicated in Table 1. The [25] report shows that relative permittivity is tenfold higher than normal tissue. The boundary conditions applied in the simulation are the Absorbing Boundary Conditions (ABC), Perfect Match Layer (PML), and Perfect Electric Conductor (PEC). PML is a type of ABC used to minimize reflection at the outer simulation domain boundary.PEC is used to model perfect conductors such as metal surfaces or the boundary of the simulation domain. It also ensures that EM waves entirely reflect without penetrating the conductive surface. The tangential E field components on the outer boundary are set to 0.

The relationship between frequency and dielectric property is expressed in Eq.(11). The dispersive material model assigns breast fat, tumor, and muscle with frequency-dependent dielectric properties. The material responses to wave frequency are flexibly and computationally manageable[26].

In this simulation with SEMCAD, a generic model is used as a dispersive material model, which integrates with Drude, Debye and Lorentz. The Generic Dispersive Model (GDM) is expressed in (12-12a) [20]. GDM describes the frequency-dependent behavior of permittivity material with applied frequency. The dielectric properties are listed in Table 1.

$$f=\frac{c}{\lambda\sqrt{\varepsilon_r \mu_r}}. \quad (11)$$

$$\varepsilon(\omega) = \varepsilon(\infty) - j\frac{\sigma}{\omega\varepsilon_o} + GDM \tag{12}$$

$$\varepsilon(\omega) = \varepsilon(\infty) - j\frac{\sigma}{\omega\varepsilon_o} + \sum_{P=1}^{P}\frac{A}{B\omega^2 + Cj\omega + D} \tag{12a}$$

Where $\varepsilon(\omega)$=complex relative permittivity regarding angular frequency
$\varepsilon_o = 8.85x10^{-15}F/m$
σ = electrical conductivity
$\omega = 2\pi f$
P= no of poles
$\varepsilon(\infty)$ = for permittivity $\omega \to \infty$
A,B,C,D = coefficient for Generic Dispersive Model

The GDM employs linear dispersion [27], which refers to the material's relationship between frequency (wavelength) and EM wave propagation. In SEMCAD X, linear dispersion was added with electric poles. Assume there is no magnetic dispersive pole. There are three dispersive poles in 434MHz, 915MHz and 2450MHz. ABCD is the coefficient used as a fitting parameter to obtain better-fit data. Tables 2 to 4 represent the coefficient of GDM for tumors with 434MHz, 915MHz and 2450MHz applicators, respectively.

Table 1
Tissue Permittivity and Conductivity

	Frequency (MHz)					
Tissue	434		915		2450	
	ε_r	σ (S/m)	ε_r	σ (S/m)	ε_r	σ (S/m)
Breast Fat	3.987	0.570	3.413	0.651	3.126	0.892
Tumor	55.224	1.200	43.273	4.738	16.082	33.741
Chest Wall	51.887	5.942	28.790	12.883	13.708	35.728

Table 2
GDM poles coefficient at frequency 434MHz -Tumor

Electric Pole	A	B	C	D
1	$-1.72x10^{19}$	-1	$2.38x10^{9}$	$1.18x10^{13}$
2	$-2.18x10^{22}$	-1	$3.23x10^{10}$	$2.72x10^{15}$
3	$-3.14x10^{18}$	-1	$2.61x10^{8}$	$2.97x10^{17}$

Table 3
GDM poles coefficient at frequency 915MHz -Tumor

Electric Pole	A	B	C	D
1	$6.73x10^{19}$	-1	$2.38x10^{8}$	$5.52x10^{13}$
2	$-3.62x10^{22}$	-1	$3.93x10^{10}$	$3.45x10^{15}$
3	$-8.76x10^{19}$	-1	$7.35x10^{8}$	$3.21x10^{14}$

Table 4
GDM poles coefficient at frequency 2450MHz -Tumor

Electric Pole	A	B	C	D
1	$-9.88x10^{22}$	-1	$5.81x10^{10}$	$3.47x10^{15}$
2	$3.37x10^{21}$	-1	$8.02x10^{9}$	$1.70x10^{21}$
3	$-1.12x10^{20}$	-1	7.18x109	$1.44x10^{15}$

2.3 Specific Absorption Rate

The tissue properties required to solve specific absorption rates are permittivity, electric conductivity and density. Complex permittivity has real and imaginary parts. $\varepsilon_c = \varepsilon' - j\varepsilon''$. The real part ε' related to the storage of energy, while the imaginary part, ε'' is related to loss of energy due to conductivity. The relationship between complex and relative permittivity is stated in the following equation:

$$\varepsilon_c = \varepsilon_r \varepsilon_o - j\frac{\sigma}{\omega} \tag{13}$$

The interaction between EM waves in tissue-generated heat and heat absorption in treated tissue is presented based on Specific Absorption Rate (SAR) results. Specific Absorption Rate (SAR) represents the measurement of the level of heat absorption in mass biological tissue in W/kg or mW/g[28]. SAR described[29][30] as in Eq. (13)

$$SAR = \frac{\sigma}{\rho}|E|^2 = \frac{\sigma_s + \omega\varepsilon''}{\rho}|E|^2 = \frac{\sigma_s + 2\pi f\varepsilon''}{\rho}|E|^2 \tag{14}$$

The equivalent of conductivity is σ= $\sigma_s + \omega\varepsilon''$ and σ_s = static (electrical conductivity of tissue at f=0Hz, $\omega\varepsilon''$=alternating current (electrical conductivity varies with frequency), ρ is the tissue density (kg/m^3), E= field intensity.

SAR measurement typically averages over a 1g and 10g cubic tissue volume as specified by IEEE and IEC[31]. This simulation utilized average SAR measurement over 1g tissue volume. The SAR results are recorded in the next section.

3. Results and Discussions

Figures 4, 5, and 6 display the simulation results on SAR distribution, penetration depth (PD), and SAR peak spatial with an applicator 434MHz,915MHz and 2450MHz, respectively.

The SAR distribution refers to heat distribution within the tissue, ensuring the heat distribution does not exceed the healthy surrounding tissue. PD is also called skin depth. PD is the effective distance of EM radiation travel along the skin surface to the interior. The SAR peak is spatial and represents the highest SAR value within the tumor.

The SAR distribution varies across different regions in breast phantom at distinct frequencies. The SAR distribution for the applicator with 434MHz covers the middle to the near chest wall. Meanwhile, the 915MHz applicator covers the middle region of the breast, while the 2450MHz SAR distribution is near the areola.

The SAR distribution shows that the applicator 2450MHz can focus more on the tumor near the areola. While the 915MHz applicator concentrated more on the tumor in the middle of the breast phantom, 434 MHz can be proposed for deep-seated tumors since the SAR distribution covers the middle to the near chest wall.

The relationship between wavelength and frequency is f =c/λ. At low frequencies, waves exhibit long wavelengths that enable them to propagate over long distances compared to high frequencies. This phenomenon can be associated with PD, where the low frequency can cover long distances compared to the high frequency, as illustrated in Figure 7. The simulation of the applicator at 2450MHz (high frequency) reduces PD, causing the skin adjacent to the applicator to absorb more heat. Prolonged exposure at this frequency may lead to skin burns[33]. Meanwhile, the PD for 434MHz is 90.5mm, the PD for 915MHz is 71.7mm and 15.4mm for 2450MHz. The results show that the PD is inversely proportional to the frequency. Also observed in [32] is that the PD decreases as the frequency increases. The relationship of skin depth (δ) / PD with frequency stated in this equation, PD= $\sqrt{\frac{1}{\pi\sigma\mu f}}$ [30].

The SAR peak spatial value is 70.2mW/g at 2450MHz. Comparatively, at 915MHz, it is 24.667mW/, while at 434MHz, it is 0.125mW/g. As stated in Eq. (14), the pattern of peak spatial SAR is proportional to the frequency.

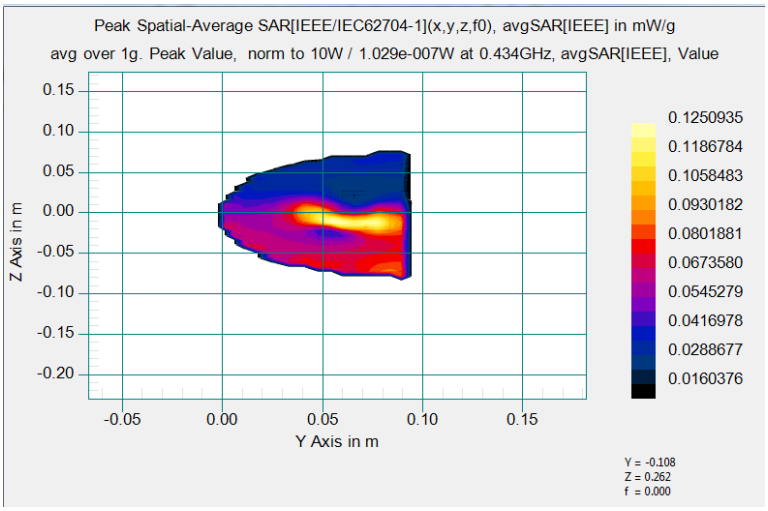

Fig. 4. SAR distribution for applicator 434MHz(PD=90.5mm)

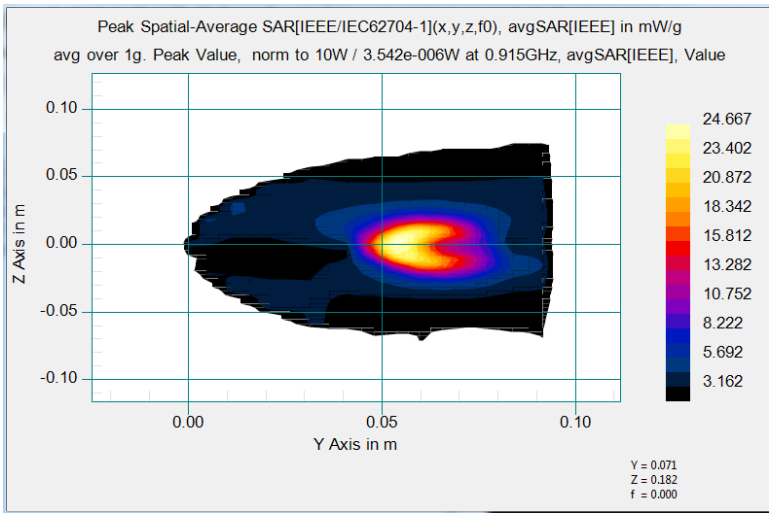

Fig. 5. SAR distribution for applicator 915 MHz(PD=71.7mm)

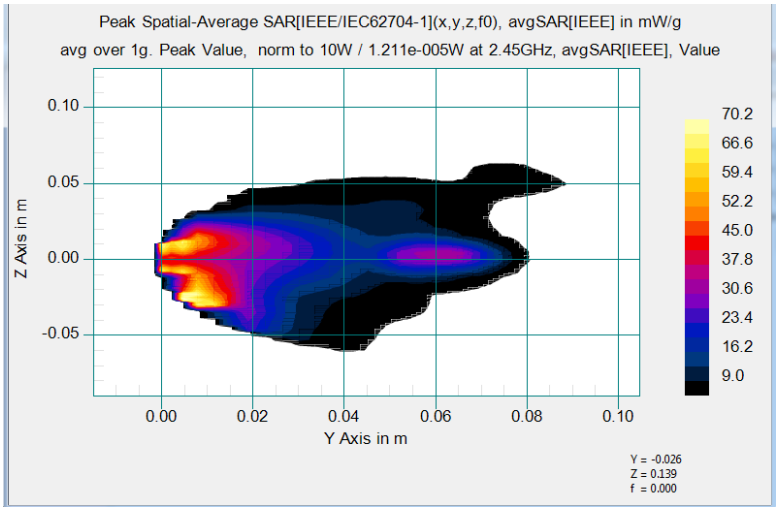

Fig. 6. SAR distribution for applicator 2450 MHz(PD=15.4mm)

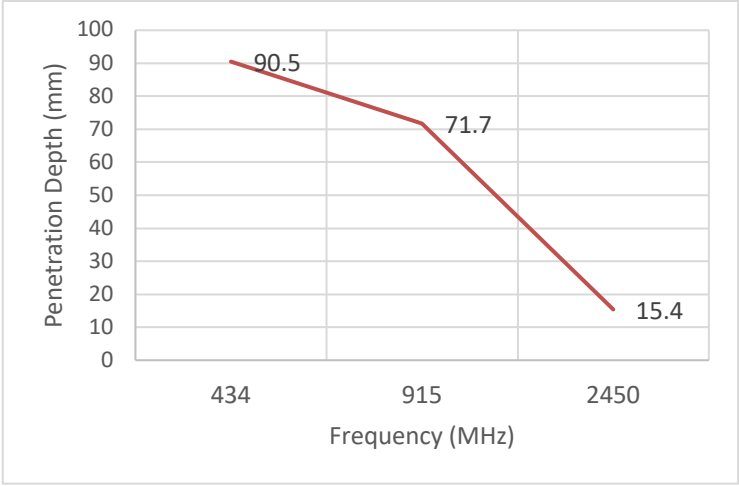

Fig. 7. The relationship between PD and frequency

4. Conclusions

In this paper, the 915MHz applicator is the suitable frequency based on the tumor location in the middle of the breast phantom. The applicator with 434MHz is suitable for deep-seated tumors, while the 2450MHz applicator suggests superficial tumors. The results are aligned with the relationship of skin depth (δ) / PD with frequency, where the low frequency can cover long distances in contrast to the high frequency.

Acknowledgement

The author gratefully acknowledges UNIMAS and UiTM for their support in the facility and guidance throughout his research. This research was not funded by any grant.

References

[1] Al Tameemi, Wafaa, Tina P. Dale, Rakad M. Kh Al-Jumaily, and Nicholas R. Forsyth. "Hypoxia-modified cancer cell metabolism." *Frontiers in cell and developmental biology* 7 (2019):. .https://doi.org/10.3389/fcell.2019.00004

[2] Harris, Bill, Sana Saleem, Natalie Cook, and Emma Searle. "Targeting hypoxia in solid and haematological malignancies." *Journal of Experimental & Clinical Cancer Research* 41, no. 1 (2022): 318. https://doi.org/10.1186/s13046-022-02522-y

[3] Emami Nejad, Asieh, Simin Najafgholian, Alireza Rostami, Alireza Sistani, Samaneh Shojaeifar, Mojgan Esparvarinha, Reza Nedaeinia et al. "The role of hypoxia in the tumor microenvironment and development of cancer stem cell: a novel approach to developing treatment." *Cancer Cell International* 21, no. 1 (2021): 1-26.. https://doi.org/10.1186/s12935-020-01719-5

[4] Begg, Katheryn, and Mahvash Tavassoli. "Inside the hypoxic tumour: reprogramming of the DDR and radioresistance." *Cell Death Discovery* 6, no. 1 (2020): 77.. https://doi.org/10.1038/s41420-020-00311-0

[5] Yildiz, Gulsah, Iman Farhat, Lourdes Farrugia, Julian Bonello, Kristian Zarb-Adami, Charles V. Sammut, Tuba Yilmaz, and Ibrahim Akduman. "Comparison of microwave hyperthermia applicator designs with fora dipole and connected array." *Sensors* 23, no. 14 (2023): 6592.https://doi.org/10.3390/s23146592

[6] Behrouzkia, Zhaleh, Zahra Joveini, Behnaz Keshavarzi, Nazila Eyvazzadeh, and Reza Zohdi Aghdam. "Hyperthermia: how can it be used?." *Oman medical journal* 31, no. 2 (2016): 89.https://doi.org/10.5001/omj.2016.19

[7] Song, C. W., H. J. Park, Chung K. Lee, and R. Griffin. "Implications of increased tumor blood flow and oxygenation caused by mild temperature hyperthermia in tumor treatment." *International Journal of Hyperthermia* 21, no. 8 (2005): 761-767.https://doi.org/10.1080/02656730500204487

[8] Kok, H. Petra, Erik NK Cressman, Wim Ceelen, Christopher L. Brace, Robert Ivkov, Holger Grüll, Gail Ter Haar, Peter Wust, and Johannes Crezee. "Heating technology for malignant tumors: A review." *International Journal of Hyperthermia* 37, no. 1 (2020): 711-741.https://doi.org/10.1080/02656736.2020.1779357

[9] Abdel-Haleem, Maha R., Tamer Abouelnaga, Mohammed Abo-Zahhad, and Sabah M. Ahmed. "A Preclinical System for Enhancing the Efficiency of Microwave Breast Cancer Hyperthermia Therapy Using Dielectric Matched Layer and Convex Lenses." *Progress In Electromagnetics Research C* 109 (2021): 153-168.https://doi.org/10.2528/PIERC20101406

[10] Rossmann, Christian, and Dieter Haemmerich. "Review of temperature dependence of thermal properties, dielectric properties, and perfusion of biological tissues at hyperthermic and ablation temperatures." *Critical Reviews™ in Biomedical Engineering* 42, no. 6 (2014). https://doi.org/10.1615/CritRevBiomedEng.2015012486

[11] Gabriel, Sami, R. W. Lau, and Camelia Gabriel. "The dielectric properties of biological tissues: II. Measurements in the frequency range 10 Hz to 20 GHz." *Physics in medicine & biology* 41, no. 11 (1996): 2251.. https://doi.org/10.1088/0031-9155/41/11/002

[12] Paulides, M. M., H. Dobsicek Trefna, S. Curto, and D. B. Rodrigues. "Recent technological advancements in radiofrequency-andmicrowave-mediated hyperthermia for enhancing drug delivery." *Advanced drug delivery reviews* 163 (2020): 3-18. https://doi.org/10.1016/j.addr.2020.03.004

[13] Altintas, Gulsah, Ibrahim Akduman, Aleksandar Janjic, and Tuba Yilmaz. "A Novel Approach on Microwave Hyperthermia." *Diagnostics* 11, no. 3 (2021): 493.https://doi.org/10.3390/diagnostics11030493

[14] Lyu, Cheng, Wenxing Li, Si Li, Yunlong Mao, and Bin Yang. "Design of Ultra-Wideband Phased Array Applicator for Breast Cancer Hyperthermia Therapy." *Sensors* 23, no. 3 (2023): 1051.https://doi.org/10.3390/s23031051

[15] Choudhary, Rahul, and Kavitha Arunachalam. "Design and comparison of semi-ellipsoidal and conical phased array applicators operating at 434 MHz for hyperthermia treatment of locally advanced breast cancer." In *2022 IEEE Region 10 Symposium (TENSYMP)*, pp. 1-3. IEEE, 2022.https://doi.org/10.1109/TENSYMP54529.2022.9864401

[16] Gupta, R. Chandra, and S. P. Singh. "Analysis of the SAR distributions in three-layered bio-media in direct contact with a water-loaded modified box-horn applicator." *IEEE Transactions on microwave Theory and techniques* 53, no. 9 (2005): 2665-2671.https://doi.org/10.1109/TMTT.2005.854209

[17] Li, Jianian, Baosheng Wang, Dajun Zhang, Chenzhe Li, Yihui Zhu, Yi Zou, Baile Chen, Tao Wu, and Xiong Wang. "A preclinical system prototype for focused microwave breast hyperthermia guided by compressive thermoacoustic tomography." *IEEE Transactions on Biomedical Engineering* 68, no. 7 (2021): 2289-2300.. https://doi.org/10.1109/TBME.2021.3059869

[18] Akimov, Yuriy. "Theory of Electromagnetic Fields." In *Emergent Micro-and Nanomaterials for Optical, Infrared, and Terahertz Applications*, pp. 23-60. CRC Press, 2022.. https://doi.org/10.1201/9781003202608-2

[19] Popov, Evgeny. *GratinGs: theory and numeric applications*. Popov, Institut Fresnel, 2012..

[20] SEMCAD, X. "Reference Guide." (2012).

[21] Rana, Md Sohel, Bijoy Kumer Sen, Md Tanjil-Al Mamun, Md Shahriar Mahmud, and Md Mostafizur Rahman. "A 2.45 GHz microstrip patch antenna design, simulation, and analysis for wireless applications." *Bulletin of Electrical Engineering and Informatics* 12, no. 4 (2023): 2173-2184.https://doi.org/10.11591/beei.v12i4.4770

[22] M. Tayel, T. Abouelnaga, and A. Elnagar, "Pencil Beam Grid Antenna Array for Hyperthermia Breast Cancer Treatment System," *Circuits Syst.*, vol. 08, no. 05, pp. 122–133, 2017, https://doi.org/10.4236/cs.2017.85008

[23] Balanis, Constantine A. *Antenna theory: analysis and design*. John wiley & sons, 2016.

[24] S. R. Avenue, "RT/duroid ® 5870 /5880," pp. 100–101.

[25] D. G. Fang, *Arrays and Array Synthesis*. 2011.

[26] Guerrero Lopez, Geshel David, Mario Francisco Jesús Cepeda Rubio, Jose Irving Hernandez Jacquez, Arturo Vera Hernandez, Lorenzo Leija Salas, Francisco Valdés Perezgasga, and Francisco Flores García. "Computational FEM model, phantom and ex vivo swine breast validation of an optimized double-slot microcoaxial antenna designed for minimally invasive breast tumor ablation: theoretical and experimental comparison of temperature, size of lesion, and SWR, preliminary data." *Computational and mathematical methods in medicine* 2017 (2017).https://doi.org/10.1155/2017/1562869

[27] Banks, Jeffrey W., Benjamin B. Buckner, William D. Henshaw, Michael J. Jenkinson, Alexander V. Kildishev, Gregor Kovačič, Ludmila J. Prokopeva, and Donald W. Schwendeman. "A high-order accurate scheme for Maxwell's equations with a generalized dispersive material (GDM) model and material interfaces." *Journal of Computational Physics* 412 (2020): 109424.. https://doi.org/10.1016/j.jcp.2020.109424

[28] Wessapan, Teerapot, Siramate Srisawatdhisukul, and Phadungsak Rattanadecho. "Specific absorption rate and temperature distributions in human head subjected to mobile phone radiation at different frequencies." *International Journal of Heat and Mass Transfer* 55, no. 1-3 (2012): 347-359.https://doi.org/10.1016/j.ijheatmasstransfer.2011.09.027

[29] Fiser, Ondrej, Ilja Merunka, and Jan Vrba. "Design, evaluation and validation of planar antenna array for breast hyperthermia treatment." In *2015 Conference on Microwave Techniques (COMITE)*, pp. 1-4. IEEE, 2015.https://doi.org/10.1109/COMITE.2015.7120228

[30] Rodrigues, Dario B., Hana Dobsicek-Trefna, Sergio Curto, Lukas Winter, Jason K. Molitoris, Jan Vrba, David Vrba, Kemal Sumser, and Margarethus M. Paulides. "Radiofrequency and microwave hyperthermia in cancer treatment." In *Principles and Technologies for Electromagnetic Energy Based Therapies*, pp. 281-311. Academic Press, 2022.. https://doi.org/10.1109/COMITE.2015.7120228

[31] I. Xplore, "IEC/IEEE 62704-1," 2017.

[32] Gao, Bin, Gaige Ru, Qiuping Ma, and Haoran Li. "Electromagnetic Multiphysics Sensing Nondestructive Testing." (2023): 101-128.. https://doi.org/10.1016/B978-0-12-822548-6.00115-1

[33] Mendez, HF Guarnizo, MA Polochè Arango, F. Coronel Rico, and IE Diaz Pardo. "Microwave Hyperthermia Study in Breast Cancer Treatment." In *2019 Congreso Internacional de Innovación y Tendencias en Ingenieria (CONIITI)*, pp. 1-5. IEEE, 2019.. https://doi.org/10.1109/CONIITI48476.2019.8960873